ION ENERGY AND ANGULAR DISTRIBUTIONS IN RF CAPACITIVELY COUPLED PLASMA SOURCES

O.V. Manuilenko, K.M. Minaeva
National Science Center "Kharkov Institute of Physics and Technology"
Kharkov, Ukraine
E-mail: ovm@kipt.kharkov.ua

The possibilities to control ion energy distribution functions (IEDFs) and ion angle distribution functions (IADFs) on electrodes in single- and dualfrequency capacitively coupled plasma (CCP) sources are investigated by means of particle-in-cell/Monte Carlo (PIC/MCC) simulations. It is shown that the IEDFs can be controlled by the driven voltage and frequency in singlefrequency capacitive discharges. It is demonstrated that the IEDFs and IADFs can be controlled by the low frequency voltage in dualfrequency CCP sources.

PACS: 52.80.-s

1. INTRODUCTION

CCP sources are widely used in the laboratory as well as in industry for a variety of processing techniques such as sputtering, plasma deposition and directional ion etching. The interaction of energetic ions with solid surfaces plays a crucial role in these techniques. The positive ions accelerated through the space-charge sheath adjacent to the electrodes are responsible for the etch rates, and the etch depths, as well as for the etch profiles. The ion bombardment energy and the ion flux on the wafer, which are important for the control of etch depths and etch rates, cannot be controlled independently by driven voltage in conventional singlefrequency CCP sources. Independent control by ion flux and ion energy is possible in the dualfrequency CCP sources [1]. Careful control of etch profiles is a basic requirement for modern etch technologies. Etch profiles are defined by the IEDF and IADF on the wafer. Collisionless IEDFs on electrodes in singlefrequency CCP sources were reviewed in [2]. PIC/MCC simulations [3-6] were used to study the possibility of IEDF control on the powered electrode in asymmetric single- and doublefrequency capacitive discharges in argon and different mixtures [7-16]. In the present paper, the possibilities to control IEDFs and IADFs on electrodes in single- and dualfrequency CCP sources are investigated by means of PIC/MCC simulations. It is shown that the IEDFs can be controlled by the driven voltage and frequency in singlefrequency CCP sources, and the IEDFs and IADFs can be controlled by the low frequency voltage in dualfrequency capacitive discharges.

2. SIMULATION TOOL AND CONDITIONS

Weakly ionized plasmas in asymmetric single- and dualfrequency CCP sources have been studied in one dimension using the bounded electrostatic 1d3v PIC/MCC code [3-6]. One dimensional plasma model can be used due to large ratio of transverse to longitudinal dimensions of conventional CCP sources. The elastic scattering, excitation, and ionization for electron-neutral collisions, the charge exchange and elastic scattering for ion-neutral collisions are included in the model via Monte Carlo. The grid size Δx was small enough to resolve Debye length. The time step Δt was less then the minimal time scale in the discharge, and $\omega_{pe}\Delta t < 0.1$, where ω_{pe} – electron plasma frequency. The "Courant condition for particles" $v\Delta t/\Delta x < 1$, where v is the velocity of the macro particle, was satisfied during modeling time. The modeling conditions are different for different runs, but the scales are following: $\Delta t \in [10^{-12}, 10^{-11}]$ sec, $\Delta x \in [4\cdot10^{-4}, 4\cdot10^{-3}]$ cm.

In conventional PIC/MCC simulations numerical fluctuations are inversely proportional to $\sqrt{N_{De} + N_{cell}}$, where N_{De} is the number of macroparticles per Debye length, and N_{cell} is the number of computer particles per cell. This numerical noise can increase the kinetic energy of the particles and creates substantial errors in the electron energy distribution function, electron temperature and plasma density. To investigate the influence of N_{cell} and N_{De} (which is proportional to N_{cell}) on the CCP source characteristics the testing simulations were done. Fig.1 shows the electron energy distribution functions measured in the centre of the discharge for $N_{cell} = 8$ (left) and $N_{cell} = 1000$ (right), respectively. The modeling done for pressure 90 mTorr, electrode spacing 1.3 cm, driven voltage 120 V, frequency 30 MHz, $\Delta x \in 4\cdot10^{-3}$ cm. As it follows from Fig. 1, the modeling with small number of macro particles can not exactly resolve two-temperature electron energy distribution functions in the capacitively coupled plasma sources.

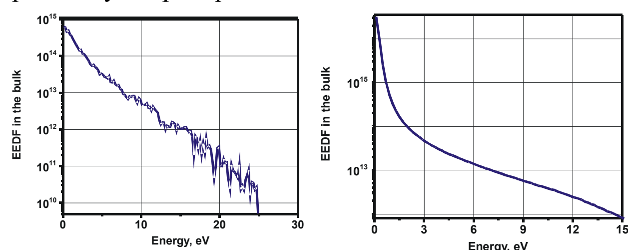

Fig.1. Electron energy distribution functions measured in the centre of the discharge for $N_{cell} = 8$ (left) and $N_{cell} = 1000$ (right), respectively

Fig.2 shows the maximal T_e^{max} and minimal T_e^{min} electron temperatures in the capacitively coupled plasma

source vs N_{cell}. As it follows from Fig.2, T_e^{min} strongly depends from N_{cell}. The maximal plasma density vs N_{cell} is presented in Fig.3. Same as for T_e^{min}, the maximal plasma density strongly depends from N_{cell}. As it follows from Figs.1-3, the N_{cell} should be higher than 250 in the conventional particle simulation. In each modeling case presented here from 250 to 1000 macro particles per cell was used in order to decrease numerical noise, which can cause substantial errors in the electron temperature, and so, in plasma density and ion flux on the wafer.

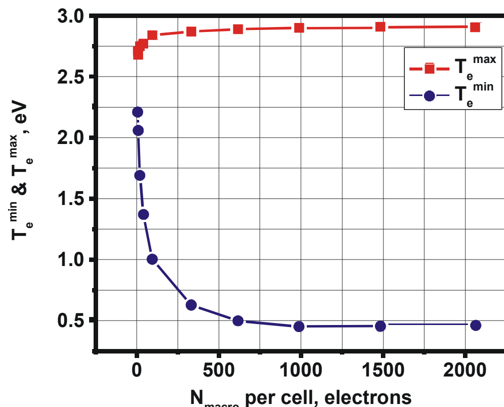

Fig.2. Maximal T_e^{max} and minimal T_e^{min} electron temperatures vs the number of macroparticles per cell N_{cell}

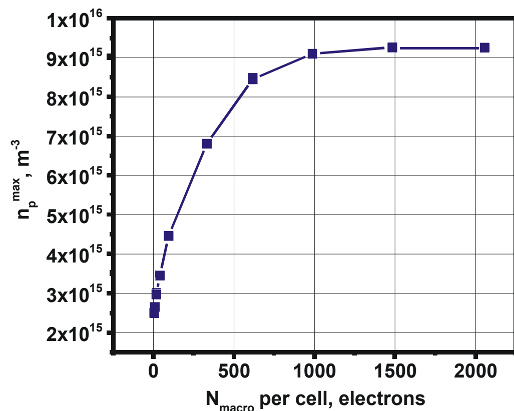

Fig.3. Maxima plasma density n_p^{max} (measured in the centre of the discharge) vs the number of computer particles per cell N_{cell}

3. RESULTS AND DISCUSSION

Figure 4 shows the IEDFs on the powered electrode for various driven voltages V_{hf} (80 V for upper graph, and 1300 V for lower graph) in the singlefrequency 30 MHz Ar discharge at 70 mTorr. As it is shown in Fig.1, the IEDFs have fine structure, which is typical for low pressure discharges under following conditions: there are few charge-exchange collisions on the sheath length, and ion transit time through sheath τ_{ion} is greater then RF period τ_{hf}. These peaks are arisen because of acceleration of slow ions, which are created in the sheath as the result of charge-exchange collisions, by varying sheath potential. It is necessary to emphasize, that the nature of the slow energy ions generation in the sheath is not important for the IEDF shape and for the spikes position. This ions can be generated, for example, by secondary electrons in ionization collisions with neutrals, or by external UV radiation.The number of peaks can be estimated as

$$N = \frac{\tau_{ion}}{\tau_{hf}} = \frac{1}{\pi\sqrt{2\eta}}, \qquad (1)$$

where $\eta = \frac{eU}{4\pi^2 M f_{hf}^2 s^2}$, $U = V_p - V_{dc}$ is the bias voltage, V_{dc} is the self-bias potential, V_p is the plasma potential, f_{hf} is the driven frequency, s is the sheath thickness, e is the ion charge, and M is the ion mass. As it follows from (1), and confirms by Fig.4, the number of peaks decreases with increasing bias voltage U and, so with increasing driven voltage V_{hf}. Thus the IEDF shape can be controlled by the applied voltage.

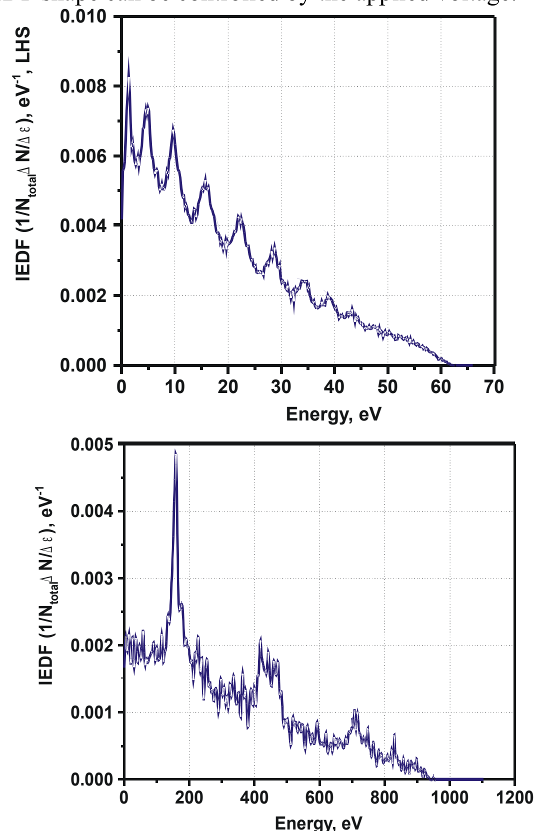

Fig.4. IEDFs on the driven electrode for two different driven voltages V_{hf} (80 V for upper graph, and 1300 V for lower graph)

Fig.5 shows time averaged spatial profiles of electron and ion densities (upper graph), and the potentials (lower graph) for different values of driven voltage V_{hf}. The maximal plasma density and ion fluxes onto elec-

trodes vs V_{hf} are presented in the inset of the Fig.5 (upper graph). The self-bias V_{dc} and plasma V_p potentials vs V_{hf} are shown in the inset of the Fig.5 (lower graph). As follows from Fig.5, the maximal plasma density and ion fluxes onto electrodes increases with V_{hf}. The plasma potential V_p and self-bias voltage V_{dc}, and so, the maximal ion energy, have almost linear dependence against V_{hf}. Thus the ion energy and ion fluxes onto electrodes can not be controlled independently by driven voltage.

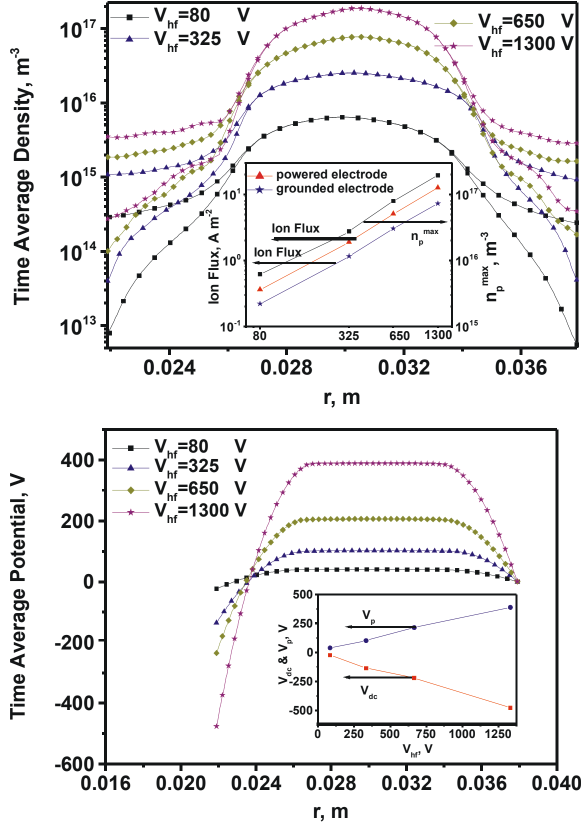

Fig.5. Time averaged spatial profiles of electron and ion densities (upper graph), and the potentials (lower graph) for different values of driven voltage V_{hf}

Fig.6 shows the IEDF on the powered electrode for two driven frequencies (30 MHz upper graph and 130 MHz lower graph) at driven voltage 1200 V and pressure 50 mTorr. The peak structures are clearly visible. As follows from (1) and the scaling law for the sheath length [8] $s \propto f_{hf}^{-0.8}$, the number of peaks depends weakly on the frequency. The IEDF changes drastically as the driven frequency increases. With the increase in frequency the relative number of high energy ions increases with a consequent decrease in the number of low energy ions. At high frequency (Fig.6, lower graph), when $\frac{s}{\lambda_i} \propto 3$, where λ_i is the ion mean free path, the IEDF exhibits a saddle-shaped structure. This structure is due to ions that have passed through the sheath without collisions. It is centred around the dc sheath voltage U. At low frequencies (Fig.6, upper graph), when $\frac{s}{\lambda_i} \propto 10$, the bimodal structure disappears. The number of peaks obtained in the modelling is in good agreement with (1). Thus the IEDF shape can be controlled by the driven frequencies.

The maximal plasma density and ion fluxes onto electrodes vs driven frequency are presented in Fig.6. As follows from Fig.7, the plasma density scales as f_{hf}^2. The plasma potential and self-bias voltage, and so, the maximal ion energy, weakly depends on frequency. That is why ion fluxes onto electrodes scales as f_{hf}^2. Thus the ion fluxes onto electrodes can be controlled by driven frequency independently from ion maximal energy.

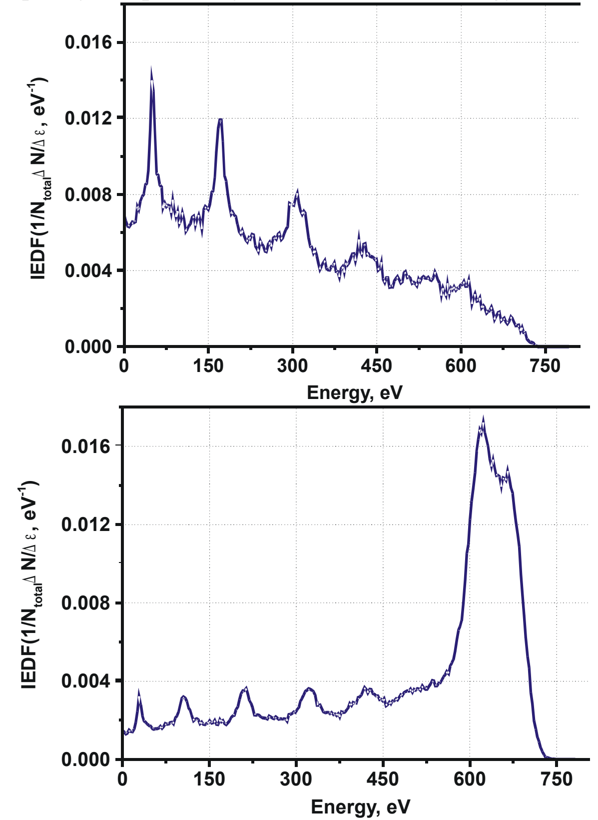

Fig.6. IEDF on the driven electrode for two frequencies (30 MHz upper graph and 130 MHz lower graph) at driven voltage 1200 V and pressure 50 mTorr

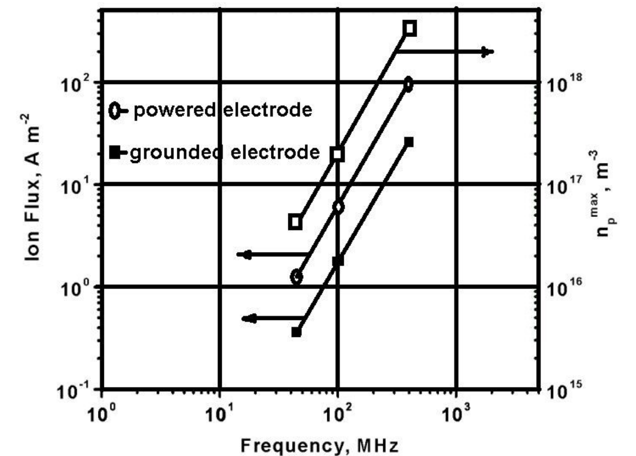

Fig.7. The maximal plasma density and ion fluxes onto electrodes vs driven frequency at driven voltage 1200 V and pressure 50 mTorr

To control independently ion fluxes onto electrodes and ion energy, the dualfrequency CCP source is used. The plasma density and, subsequently, the ion flux can be controlled by the high frequency RF power. The ion bombardment energy on the surface is defined by the low frequency (LF) power. The IEDFs on the powered electrode for two diferent LF (2 MHz) voltages (20 V for upper graph and 250 V for lower graph) at high frequency (30 MHz) voltage 160 V, and Ar pressure 70 mTorr in the dualfrequency CCP source are presented in Fig. 8. The fine structure, observed in the single-frequency case (Figs.4,6), and in the case of small LF drive (Fig.8, upper graph), is destroyed as LF voltage increases (Fig.8, lower graph). This can be explained by the growth of the sheath length (Fig.9, upper graph) and, so, by increasing of the collisional parameter s/λ_i . For the upper graph in Fig.9, this parameter approximately 10, and for lower IEDF in the Fig.8, it is 20. Thus the IEDF shape can be controlled by the LF voltage. The ion bombardment energy, which is proportional to the bias voltage U , increases (Fig.9, upper graph), and maximal plasma density decreases with LF voltage (Fig.9, lower graph). The ion fluxes onto electrodes vs LF voltage are presented in Fig.9. As follows from Fig.9, the ion fluxes onto electrodes slightly depend from LF voltage. Thus the ion bombardment energy can be controled by LF voltage independently from ion fluxes onto electrodes.

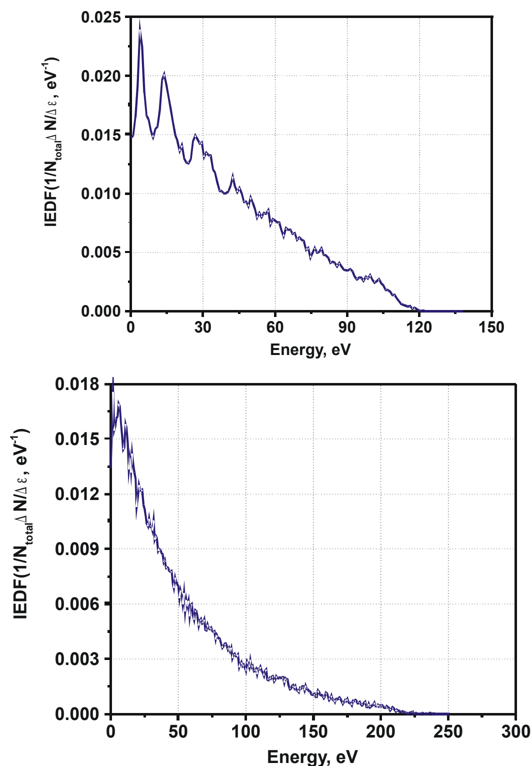

Fig.8. IEDF on the driven electrode for different LF (2 MHz) voltages (20 V for upper graph, and 250 V for lower graph). Pressure 70 mTorr, high frequency voltage 160 V, frequency 30 MHz

Fig.10 shows the IADFs on the powered electrode for various LF voltages. As follows from Fig.10, a large amount of ions strike the surface within an angle of about 3°. The IADF maximum is shifted with the LF voltage towards the low angles. The IADFs are widespread: a significant fraction of the ions impinge with highly off-normal angles.

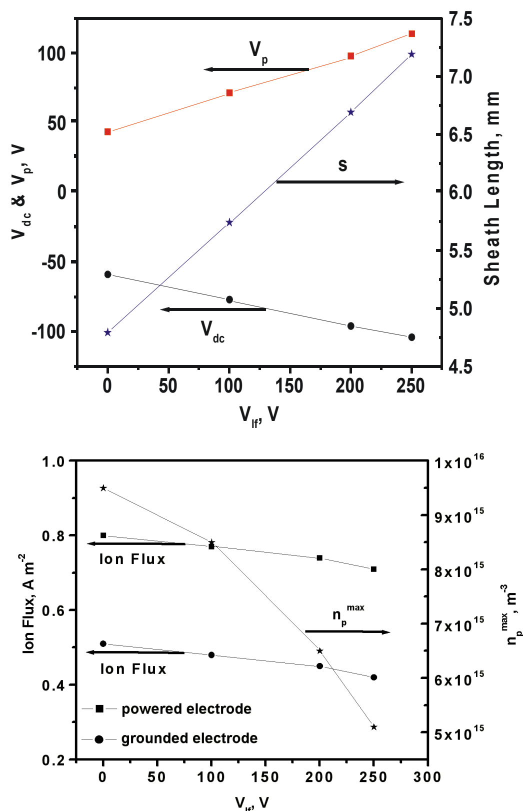

Fig.9. The self-bias potential V_{dc} , the plasma potential V_p , and the sheath length s vs LF (2 MHz) voltages (upper graph), and the maximal plasma density, and ion fluxes onto electrodes vs LF (2 MHz) voltages (lower graph)

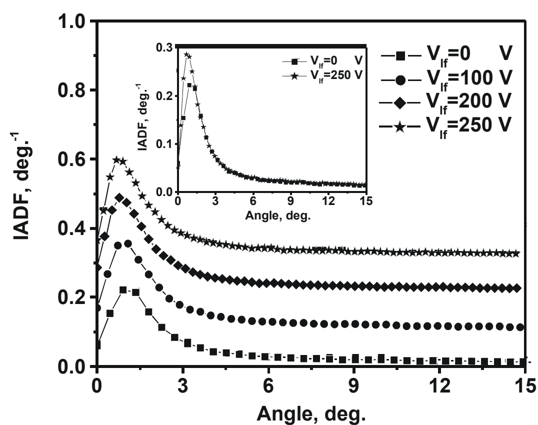

Fig.10. IADFs on the powered electrode for different LF (2 MHz) voltages. High frequency (30 MHz) voltage is 160 V, pressure 70 mTor. Vertical scales have been shifted to separate plots. Unshifted IADFs for two values of low frequency voltage are shown in the inset of the figure

The collisionless IADFs are presented in Fig.11. Charge exchange collisions and elastic scattering were

switched off in this simulation. In the collisionless case all ions strike the electrode within an angle less 3°. The IADF maximum is shifted with low frequency voltage towards the low angles.The effect of charge exchange collisions and elastic scattering can be separated (see Fig.12). Ions near normal incidence angle are created by charge exchange collisions or crossed it without collisions. Ions which hit the electrode with a larger impact angle have been scattered in the sheath. Fig.13 shows the IADF plotted for different impact energies. Ions with energy less than 10 eV have been created at the electrode by the charge exchange and ionization collisions.

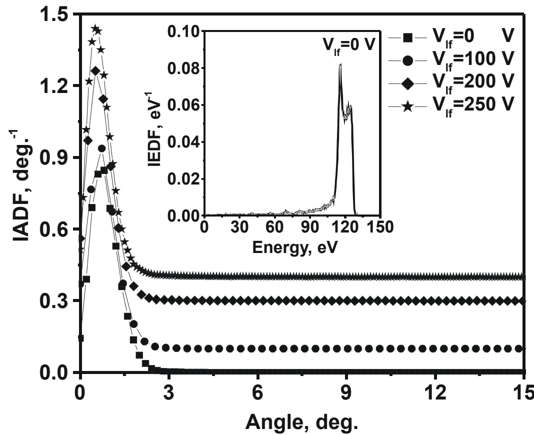

Fig.11. Collisionless IADFs on the powered electrode for different low frequency (2 MHz) voltages. High frequency voltage is 160 V, pressure 70 mTorr, frequency 30 MHz. Vertical scales have been shifted to separate plots. Collisionless two-hump IEDF is shown in the inset of the figure

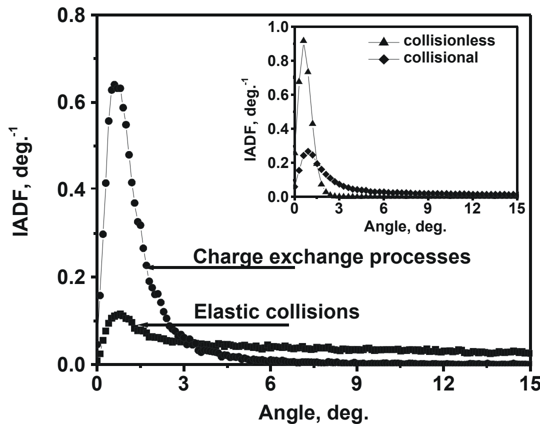

Fig.12. IADFs on the powered electrode for pressure 70 mTorr, high frequency (30 MHz) voltage 160 V, low frequency (2 MHz) voltage 150 V. Simulations were done with switched on charge exchange collisions and turned of elastic collisions and vice versa. Collisionless and collisional IADFs are shown in the inset of the figure

Typical IADFs obtained by PIC/MCC simulations are presented in Figs.10-13. The behavior of IADFs in the region of low angles can be made clear on the basis of exact calculations with the model ion velosity distribution functions on the electrode:

$$f(v_{\parallel}, v_{\perp}) = \frac{m}{2\pi\, kT_{\perp}} \cdot \sqrt{\frac{m}{2\pi\, kT_{\parallel}}} \cdot \exp\left(-\frac{mv_{\perp}^2}{2kT_{\perp}} - \frac{mv_{\parallel}^2}{2kT_{\parallel}} \right).$$

In spherical coordinates IADF is given by

$$\Gamma(\vartheta) = \int_0^{2\pi} d\varphi \int_0^{\infty} v^2 dv \int_0^{\vartheta} \sin(\vartheta) d\vartheta \left(nv\cos(\vartheta) \right) f(v, \vartheta).$$

Integral can be easy calculated:

$$\Gamma(\vartheta) = \frac{n\langle v_{\parallel}\rangle}{4} \frac{\alpha \cdot \sin^2(\vartheta)}{1 + (\alpha - 1)\cdot \sin^2(\vartheta)},$$

where $\langle v_{\parallel}\rangle = \sqrt{\frac{8kT_{\parallel}}{\pi\, m}}$, $\alpha = \frac{T_{\parallel}}{T_{\perp}}$. For $\alpha = 1$ and $\vartheta = \frac{\pi}{2}$ we obtain well known result: $\Gamma_o = \frac{n\langle v\rangle}{4}$. The IADF is defined as probability density function $d\Gamma(\vartheta)$:

$$d\Gamma(\vartheta) = \frac{n\langle v_{\parallel}\rangle}{4} \frac{2\alpha \cdot \sin(\vartheta)\cos(\vartheta) d\vartheta}{(1 + (\alpha - 1)\cdot \sin^2(\vartheta))^2}.$$

Fig.14 shows normalized to Γ_o probability density functions $d\Gamma(\vartheta)$ for various values of α. As follows from Fig.14, and analitical expression for $d\Gamma(\vartheta)$, when $\vartheta \to 0$ the $d\Gamma(\vartheta) \to 0$. When $\alpha >> 1$ the angular distribution is anisotropic and most ions impact the electrode with near-normal incidence.

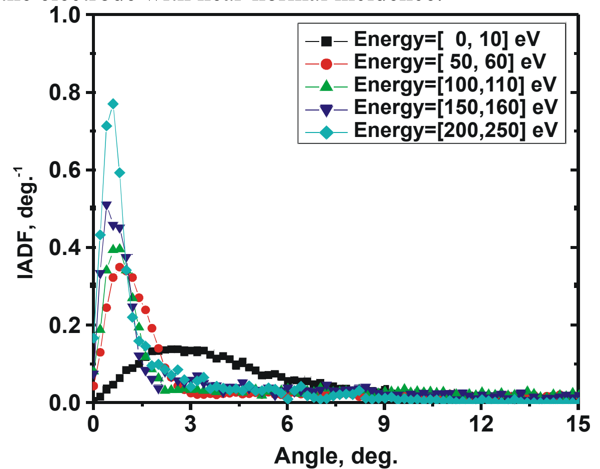

Fig.13. Energy resolved IADF for pressure 70 mTorr, high frequency voltage 160 V, low frequency voltage 150 V

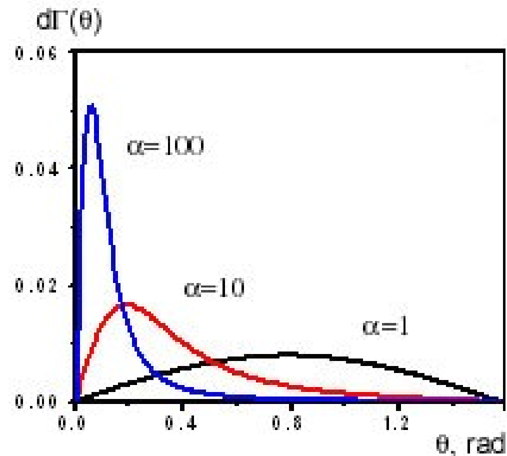

Fig.14. Normalized ion probability density functions for various values of $\alpha = T_{\parallel}/T_{\perp}$

In conclusion, the IEDF on the powered electrode in asymmetric single- and doublefrequency driven capacitive discharges in argon has been investigated with

PIC/MCC simulations. It has been demonstrated that the IEDF shape and width can be controlled by the driven voltage in a singlefrequency CCP. It has been found that an increase in the driven frequency leads to significant changes in the IEDF shape, increasing the relative number of high energy ions and decreasing the number of low energy ions. The IEDF width does not change if the frequency increases. It has been demonstrated that the width of the IEDF is increased by growth of the lowfrequency voltage in a doublefrequency CCP, and the fine structure observed in the singlefrequency case disappears simultaneously.

REFERENCES

1. R.J. Shul and S.J. Pearton. *Handbook of Advanced Plasma Processing Techniques.* Berlin: "Springer", 2000.
2. E. Kawamura, V. Vahedi, M.A. Lieberman and C.K. Birdsall. Ion Energy Distributions in RF Sheaths // *Plasma Sources Science and Technology.* 1999, v.8, №1, p.R45-R61.
3. C.K. Birdsall and A.B. Langdon. *Plasma Physics via Computer Simulation.* N.-Y.: "Hilger", 1991.
4. C.K. Birdsall. Particle-in-Cell Charged-Particle Simulations, Plus Monte Carlo Collisions with Neutral Atoms, PIC-MCC // *IEEE Transactions on Plasma Science.* 1991, v.19, №1, p.65-85.
5. V. Vahedi, G. DiPeso, C.K. Birdsall, M.A. Lieberman, T.D. Rognlien. Capacitive RF Discharges Modelled by Particle-in-Cell Monte Carlo Simulation. I. Analysis of Numerical Techniques // *Plasma Sources Science and Technology.* 1993, v.2, №3, p.261-272.
6. V. Vahedi, G. DiPeso, C.K. Birdsall, M.A. Lieberman, T.D. Rognlien. Capacitive RF Discharges Modelled by Particle-in-Cell Monte Carlo Simulation. II. Comparisons with Laboratory Measurements of EEDFs //*Plasma Sources Science and Technology.* 1993, v.2, №3, p.273-278.
7. J.K. Lee, N.Y. Babaeva, O.V. Manuilenko, H.C. Kim, J.W. Shon. Simulation of Capacitively Coupled Single- and Dualfrequency RF Discharges // *IEEE Transactions on Plasma Science.* 2004, v.32, №1, p.47-53.
8. J.K. Lee, O.V. Manuilenko, N.Y. Babaeva, H.C. Kim, J.W. Shon. Ion energy distribution control in single- and dualfrequency capacitive plasma sources // *Plasma Sources Science and Technology.* 2005, v.14, №1, p.89-97.
9. H.C. Kim, O.V. Manuilenko, J.K. Lee. Particle-In-Cell Monte-Carlo Simulation of Capacitive RF Discharges: Comparison with Experimental Data // *Japanese Journal of Applied Physics.* 2005, v.44, №4A, p.1957-1958.
10. O.V. Manuilenko, N.Y. Babaeva, H.C. Kim, J.K. Lee. *Dualfrequency capacitively coupled discharges: theories and modelings*. Abstracts of 7-th Asia Pacific Conference on Plasma Science and Technology and 17-th Symposium on Plasma Science for Materials. Fukuoka, Japan. 2004, p.59.
11. J.K. Lee, O.V. Manuilenko, N.Y. Babaeva, et al. *PIC/MCC simulation and analytical models of single- and dualfrequency capacitive RF discharges*. Proc. of SEMICON Korea Technology Symposium 2004. Seoul, S. Korea. p.11-27.
12. J.K. Lee, S.S. Yang, H.C. Kim, S.W. Ko, N.Y. Babaeva, O.V. Manuilenko, T.R. Chung, J.W. Shon. Simulations of plasma display panels and capacitively coupled plasmas // *XXVI-th International Conference on Phenomena in Ionized Gases. Greifswald, Germany, July 15-20, 2003, Conf. proc.,* v.3, p.15.
13. J.K. Lee, H.C. Kim, N.Y. Babaeva, O.V. Manuilenko, J.W. Shon. Simulations of capacitively coupled single- and dualfrequency RF discharges // *30-th IEEE International Conference on Plasma Science. Jeju, S. Korea, June 2-5, 2003, Abstracts,* p.458.
14. V. Georgieva, A. Bogaerts. Numerical simulation of dual frequency etching reactors: Influence of the external process parameters on the plasma characteristics // *Journal of Applied Physics.* 2005, v.98, №8, p.023308.
15. V. Georgieva, A. Bogaerts. *Numerical study of an Ar/CF4/N2 discharge in an asymmetric dual frequency reactor.* Proc. of XXVII-th International Conference on Phenomena in Ionized Gases. Eindhoven, the Netherlands. 2005, v.1, p.85.
16. F.F. Chen. *RF Plasma Sources for Semiconductor Processing. Advanced Plasma Technology.* N.-Y.: "Wiley", 2006.

ФУНКЦИИ РАСПРЕДЕЛЕНИЯ ИОНОВ ПО ЭНЕРГИЯМ И УГЛАМ В ИСТОЧНИКАХ ПЛАЗМЫ НА ОСНОВЕ ВЫСОКОЧАСТОТНОГО ЁМКОСТНОГО РАЗРЯДА

О.В. Мануйленко, Е.М. Минаева

С помощью численного моделирования методом макрочастиц изучены возможности управления функциями распределения ионов по энергиям и углам на электродах в одно- и двухчастотном источниках плазмы на основе ёмкостного разряда. Показано, что функциями распределения ионов по энергиям можно управлять с помощью амплитуды и частоты высокочастотной накачки, поддерживающей разряд в одночастотном источнике плазмы. Показано также, что функциями распределения ионов по энергиям и углам можно управлять с помощью величины амплитуды низкочастотного сигнала в источнике плазмы на основе двухчастотного ёмкостного разряда.

ФУНКЦІЇ РОЗПОДІЛУ ІОНІВ ЗА ЕНЕРГІЯМИ ТА КУТАМИ У ДЖЕРЕЛАХ ПЛАЗМИ НА ОСНОВІ ВИСОКОЧАСТОТНОГО ЄМКІСНОГО РОЗРЯДУ

О.В. Мануйленко, К.М. Мінаєва

За допомогою числового моделювання методом макрочастинок досліджено можливості керування функціями розподілу іонів за енергіями та кутами на електродах у одно- та двухчастотних джерелах плазми на основі ємкісного розряду. Показано, що функціями розподілу іонів за енергіями можна керувати за допомогою амплітуди та частоти високочастотної накачки, яка підтримує розряд у одночастотному джерелі плазми. Показано також, що функціями розподілу іонів за енергіями та кутами можна керувати за допомогою амплітуди низькочастотного сигналу у джерелі плазми на основі двухчастотного ємкісного розряду.